Developmental Cell
Article

# PI3K Class II α Controls Spatially Restricted Endosomal PtdIns3*P* and Rab11 Activation to Promote Primary Cilium Function

Irene Franco,[1,7] Federico Gulluni,[1,7] Carlo C. Campa,[1,7] Carlotta Costa,[1,7,8] Jean Piero Margaria,[1] Elisa Ciraolo,[1] Miriam Martini,[1] Daniel Monteyne,[2] Elisa De Luca,[1] Giulia Germena,[1] York Posor,[3] Tania Maffucci,[4] Stefano Marengo,[1] Volker Haucke,[3] Marco Falasca,[4] David Perez-Morga,[2,5] Alessandra Boletta,[6] Giorgio R. Merlo,[1] and Emilio Hirsch[1,*]
[1]Molecular Biotechnology Center, Department of Molecular Biotechnology and Health Sciences, University of Torino, 10126 Torino, Italy
[2]Laboratoire de Parasitologie Moléculaire, Institut de Biologie et de Médecine Moléculaires (IBMM), Université Libre de Bruxelles, Gosselies, 6041 Charleroi, Belgium
[3]Leibniz Institut für Molekulare Pharmakologie, 13125 Berlin, Germany
[4]Centre for Diabetes, Blizard Institute, Barts and The London School of Medicine and Dentistry, Queen Mary University of London, London E1 2AT, UK
[5]Center for Microscopy and Molecular Imaging-CMMI, Université Libre de Bruxelles, 8 rue Adrienne Bolland, 6041 Gosselies, Belgium
[6]Division of Genetics and Cell Biology, Dibit San Raffaele Scientific Institute, 20132 Milan, Italy
[7]These authors contributed equally to this work
[8]Present address: Massachusetts General Hospital Cancer Center, Harvard Medical School, Charlestown, MA 02129, USA
*Correspondence: emilio.hirsch@unito.it
http://dx.doi.org/10.1016/j.devcel.2014.01.022

## SUMMARY

**Multiple phosphatidylinositol (PtdIns) 3-kinases (PI3Ks) can produce PtdIns3*P* to control endocytic trafficking, but whether enzyme specialization occurs in defined subcellular locations is unclear. Here, we report that PI3K-C2α is enriched in the pericentriolar recycling endocytic compartment (PRE) at the base of the primary cilium, where it regulates production of a specific pool of PtdIns3*P*. Loss of PI3K-C2α-derived PtdIns3*P* leads to mislocalization of PRE markers such as TfR and Rab11, reduces Rab11 activation, and blocks accumulation of Rab8 at the primary cilium. These changes in turn cause defects in primary cilium elongation, Smo ciliary translocation, and Sonic Hedgehog (Shh) signaling and ultimately impair embryonic development. Selective reconstitution of PtdIns3*P* levels in cells lacking PI3K-C2α rescues Rab11 activation, primary cilium length, and Shh pathway induction. Thus, PI3K-C2α regulates the formation of a PtdIns3*P* pool at the PRE required for Rab11 and Shh pathway activation.**

## INTRODUCTION

Phosphatidylinositol 3-kinases (PI3Ks) are lipid kinases involved in a large set of biological processes, including membrane receptor signaling, cytoskeletal organization, and endocytic trafficking (Ghigo et al., 2010; Vanhaesebroeck et al., 2010). Mammals possess eight PI3K genes, which are divided into three classes on the basis of structural homology and substrate specificity (class I, II, and III). All PI3Ks phosphorylate the D3 position of the inositol ring of phosphatidylinositols (PtdIns), lipids involved in signal transduction as well as in membrane specification and dynamics (Di Paolo and De Camilli, 2006). Of the different 3-phosphorylated PtdIns species, PtdIns3*P* is the only product that can be directly or indirectly generated by all PI3K classes in vivo (Jean and Kiger, 2012). For example, class I PI3Ks (PI3Kα, PI3Kβ, PI3Kγ, and PI3Kδ) produce PtdIns(3,4,5)$P_3$ that can be converted into PtdIns3*P* by phosphatases acting on endocytic vesicles (Shin et al., 2005). The unique member of class III, Vps34, is responsible for a major fraction of PtdIns3*P* produced on endocytic vesicles, where it controls the generation of autophagosomes (Backer, 2008) as well as docking and fusion of endosomes (Christoforidis et al., 1999). Class II PI3Ks (namely, PI3K-C2α, PI3KC2β, and PI3KC2γ) produce PtdIns3*P* as well (Falasca et al., 2007; Maffucci et al., 2003) and are involved in intracellular membrane trafficking, endocytosis, exocytosis (Falasca and Maffucci, 2012), and autophagy (Devereaux et al., 2013). However, the precise function of class II PI3K-produced PtdIns3*P* remains partially obscure. In flies, the only class II homolog, Pi3k68D, is required for endosomal sorting from the endocytic compartment to the plasma membrane, likely via regulation of PtdIns3*P* levels (Jean et al., 2012; Velichkova et al., 2010). Mammalian PI3K-C2α has been proposed to play a similar role in endothelial cells, where it promotes endosomal trafficking via RhoA activation and regulation of PtdIns3*P* levels. This process is required for the targeting of vascular endothelial (VE)-cadherin to tight junctions and consequent endothelial cell maturation and vessel integrity (Yoshioka et al., 2012). In agreement with PI3K-C2α playing multiple roles in different membrane compartments, PI3K-C2α has been reported to produce PtdIns(3,4)$P_2$ at the plasma membrane. This lipid is crucial for clathrin-coated pit maturation and clathrin-mediated endocytosis (Posor et al., 2013).

Interestingly, vesicular trafficking and metabolism of phosphorylated PtdIns converge in the organization and functional maintenance of the primary cilium (Bielas et al., 2009; Jacoby

et al., 2009; Kim et al., 2010; Nachury et al., 2007). Primary cilia are versatile organelles that, in most mammalian cells, function as motile propellers or sensorial antennas to regulate cell proliferation, polarity, differentiation, and tissue organization. Primary cilia provide a separate highly regulated compartment and, for their assembly, they require influx of proteins and membranes from the cytosol (Pedersen and Rosenbaum, 2008). Targeting of components to the cilium involves polarized trafficking of vesicles originating from the Golgi and the endocytic recycling compartment (Follit et al., 2006; Hsiao et al., 2012; Pedersen and Rosenbaum, 2008; Wang et al., 2012). Biochemical and genetic approaches indicate that delivery and docking of secretory vesicles at the base of the cilium is regulated by a cascade of events involving the activation of specific small GTPases of the Rab family (Yoshimura et al., 2007). Rab8 and its activator, Rabin8, are essential for the entry of protein cargoes into the ciliary compartment, and impaired Rabin8 localization at the base of the cilium as well as defective Rabin8-dependent Rab8 activation reduces ciliary elongation (Das and Guo, 2011; Nachury et al., 2007). Targeting of Rabin8 to the ciliary base is regulated by another Rab GTPase, Rab11 (Westlake et al., 2011), a known coordinator of endosome recycling to the plasma membrane (Grant and Donaldson, 2009). At the ciliary base, Rab11 directly associates with Rabin8 and stimulates its guanine nucleotide exchange factor activity toward Rab8 (Feng et al., 2012); consequently, loss of Rab11 causes defective Rab8 activation and results in impaired ciliary elongation (Knödler et al., 2010).

Transport of components to and from the ciliary shaft is deeply interconnected with primary cilium function in signal transduction. For example, a well-organized and fully functional primary cilium is necessary for the cellular response to Sonic Hedgehog (Shh), a morphogen critically involved in vertebrate embryonic development (Goetz and Anderson, 2010). Consistently, loss of proteins involved in intraflagellar transport prevents correct primary cilium formation and has a dramatic impact on Shh signaling and mouse development (Huangfu and Anderson, 2005; Huangfu et al., 2003; Liem et al., 2012; Ocbina et al., 2011; Tran et al., 2008). Shh effectors, such as the Smoothened transmembrane protein and the Gli transcription factors, accumulate in cilia after pathway activation (Corbit et al., 2005; Ocbina et al., 2011). Translocation of these factors to the ciliary compartment is required for downstream steps of signal transduction, and alterations of this trafficking cause impairment of Shh signaling even in the presence of a fully elongated cilium (Keady et al., 2012). Genetic deletion of Smo in mouse embryos completely disrupts Hedgehog (Hh) signaling, thus impairing turning, left-right axis development, and neural tube patterning and leading to early embryonic lethality (Zhang et al., 2001).

Loss of the *Pik3c2a* gene in mouse has been reported to cause early embryonic lethality, initially ascribed to defective vasculogenesis (Yoshioka et al., 2012). Here, we show that in addition to abnormal angiogenesis, the lack of PI3K-C2α causes defective primary cilium organization as well as reduced Shh signaling. We report that this phenotype is linked to the ability of PI3K-C2α to control the production of PtdIns3*P* at the endocytic recycling compartment located at the base of the primary cilium. This specific pool of PtdIns3*P* was found to be required to activate the Rab11/Rab8 axis and promote Smo translocation to the ciliary shaft. Thus, PI3K-C2α integrates lipid signaling and Rab11 activation necessary for Shh signaling.

## RESULTS

### PI3K-C2α Localizes at the Ciliary Base

To explore the intracellular distribution of PI3K-C2α, a GFP-tagged form of the protein (GFP-PI3K-C2α) was transfected into mouse embryonic fibroblasts (MEFs) and localization was assessed by fluorescence microscopy. During interphase, GFP-PI3K-C2α was enriched at the perinuclear/pericentriolar area (Figure 1A). In G0 cells, the centrosome constitutes the cilium basal body; thus, endogenous PI3K-C2α was stained together with a centrosomal marker (γ-tubulin) and a ciliary marker (acetyl-tubulin) to analyze relative positioning. This staining failed to show any signal along the ciliary shaft but underlined a specific accumulation of PI3K-C2α in vesicular structures surrounding the ciliary basal body (Figure 1B), a region involved in primary cilium biogenesis (Kim et al., 2010). Enrichment of the protein in proximity of the base of the primary cilium was confirmed in a cell line widely used in cilium studies: the inner medullary collecting duct 3 (IMCD3) cell line. Downmodulation of *Pik3c2a* through infection with specific small hairpin RNA (shRNA) sequences (Sh1 and Sh2) severely reduced the immunofluorescence signal, thus confirming antibody specificity (Figures S1A and S1B available online).

The pericentriolar enrichment of PI3K-C2α in primary MEFs was found to colocalize with markers of the recycling compartment such as Rab11 and the transferrin receptor (TfR) (Figure 1C, top and bottom panels, respectively). In further agreement, cell fractionation experiments revealed the presence of PI3K-C2α in Rab11+ endosomes and not in Rab7+ late endosomes (Figure 1D). Altogether, immunofluorescence and fractionation experiments reveal enrichment of PI3K-C2α in the pericentriolar recycling endocytic compartment (PRE).

### PI3K-C2α Produces a Specific Pool of Perinuclear PtdIns3*P*

To explore the function of PI3K-C2α in the PRE, PI3K-C2α-deficient (*Pik3c2a*$^{-/-}$) MEFs were obtained from animals genetically modified by gene targeting in the mouse germline and showing complete ablation of PI3K-C2α (Figures S2A–S2D). First, localization of PtdIns3*P*, a phosphoinositide mainly involved in vesicular trafficking and produced by PI3K-C2α (Falasca et al., 2007; Yoshioka et al., 2012), was analyzed in primary MEFs. Interestingly, wild-type cells stained either with a PtdIns3*P*-selective GFP-FYVE fluorescent probe (Figure 2A) or with anti-PtdIns3*P* antibodies (Figure S2E) showed abundant labeling of PtdIns3*P* around the base of the cilium. By contrast, in *Pik3c2a*$^{-/-}$ MEFs, the pool of PtdIns3*P* around the ciliary base was reduced, whereas PtdIns3*P* detected in the rest of the cell did not show significant changes (Figures 2A and 2B; Figure S2E). A small but significant reduction in total PtdIns3*P* cellular levels (−21%) was also measured by high-pressure liquid chromatography (HPLC) analysis after metabolic labeling of starved *Pik3c2a*$^{-/-}$ MEFs (Figures 2C and 2D), in line with the notion that a restricted pool of PtdIns3*P* is specifically produced by PI3K-C2α.

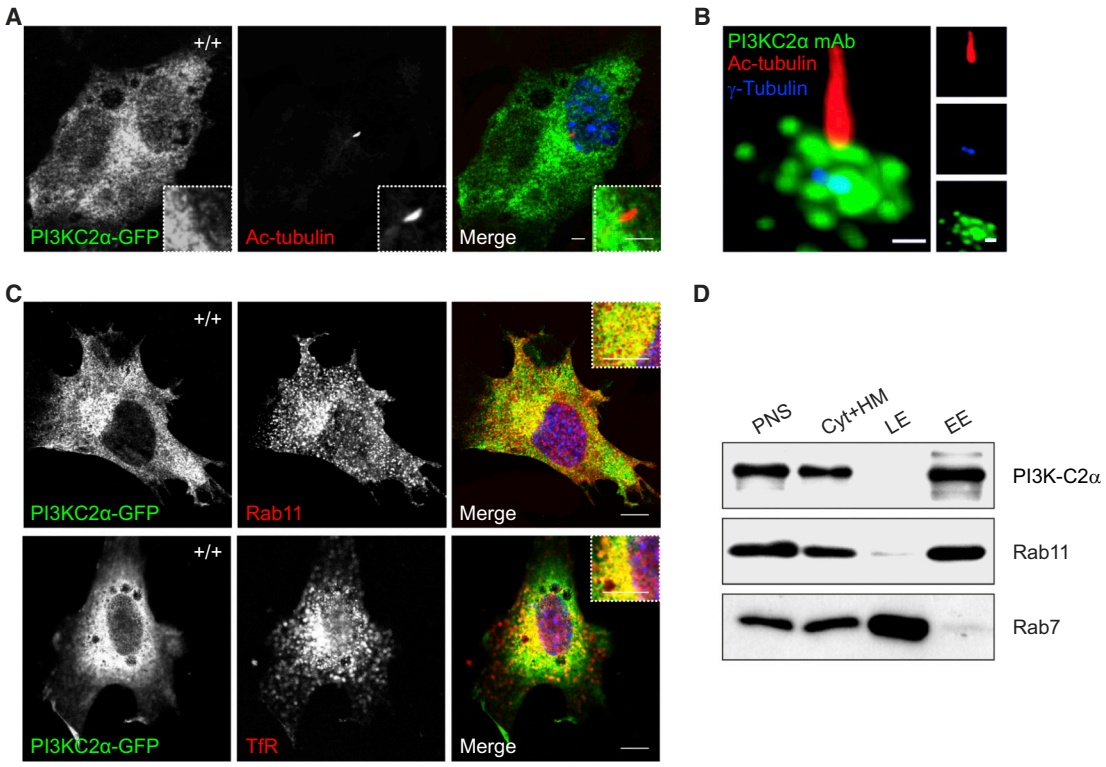


**Figure 1. PI3K-C2α Is Enriched at the Pericentriolar Recycling Compartment around the Ciliary Base**

(A) Immunofluorescence of quiescent MEFs to detect PI3K-C2α-GFP (green), acetylated α-tubulin (red), and DNA (blue), showing that transfected PI3K-C2α accumulates perinuclearly. Bar = 400 nm.

(B) Staining of the centrioles (γ-tubulin, blue), and the primary cilium (acetylated α-tubulin, red) show that endogenous PI3K-C2α (green) localizes around the ciliary base. bar = 200 nm.

(C) Costaining of PI3K-C2α-GFP (green) with markers of recycling endosomes Rab11 (red, upper panes) and transferrin receptor (TfR, red, lower panels) shows high degree of colocalization. Bar = 400 nm.

(D) Cell fractionation showing that PI3K-C2α is absent from late endosomes (LE), while it is enriched in the early endosomal (EE) and cytosol/heavy membrane fraction (Cyt+HM), similar to what observed for Rab11. PNS, postnuclear supernatant.

## Loss of PI3K-C2α Disrupts Pericentriolar Localization and Activation of Rab11

The reduction of PtdIns3*P* staining in the pericentriolar area suggested that the lack of PI3K-C2α altered the organization of the PRE compartment around the ciliary base. In agreement with this hypothesis, markers of the PRE such as Rab11 and TfR appeared dispersed and mislocalized in *Pik3c2a*$^{-/-}$ MEFs (Figures 3A and 3B, lower panels), whereas they were enriched at the expected pericentriolar location in wild-type cells. This was not due to a reduction of protein levels, because the total amount of Rab11 and TfR in *Pik3c2a*$^{-/-}$ MEFs was comparable to wild-type controls (Figures S3A and S3B). This effect was limited to recycling markers, because the early endosomal compartment was unaffected in cells lacking PI3K-C2α (Figure S3C).

To explore whether Rab11 mislocalization was related to its functional state, we analyzed Rab11 activity using a pull-down assay based on the ability of GTP-bound active Rab11 to associate with a fragment of its effector FIP3 (Eathiraj et al., 2006). The specificity of this assay was validated using a constitutively active Rab11 mutant (Rab11 Q70L) as well as Rab5 mutants as negative controls (Figure S3D). Given that *Pik3c2a*$^{-/-}$ primary MEFs scarcely proliferated in culture, Rab11 pull-down assays were performed in NIH 3T3 mouse fibroblasts infected with shRNA sequences able to significantly knock down PI3K-C2α (Sh1 and Sh2-3T3; Figure 3C). As shown in Figure 3C, reduction of PI3K-C2α expression levels significantly impaired Rab11 activation. This effect was not dependent on the cell line, because the same result could be repeated in IMCD3 (Sh1 and Sh2-IMCD3) and HeLa cells (Sh1 HeLa; Figure S3E). Overall, these data show a specific involvement of PI3K-C2α upstream of Rab11 localization and activation.

## Localization and Activation of Rab11 Require PI3K-C2α-Dependent PtdIns3P Pools

To better characterize the role of PI3K-C2α in the PRE compartment, *Pik3c2a*$^{-/-}$ MEFs were engineered to express either a kinase-inactive form of PI3K-C2α (PI3K-C2α$^{KD}$) or a PI3K-C2α mutant (PI3K-C2α$^{cIII}$) that can produce PtdIns3*P*, but not PtdIns(3,4)$P_2$ (Posor et al., 2013). Expression of either wild-type or PI3K-C2α$^{cIII}$ mutant restored accumulation of Rab11 at the pericentriolar compartment, whereas PI3K-C2α$^{KD}$ did not produce any rescue (Figure 4A). These experiments similarly restored TfR perinuclear localization only in the presence of the PI3K-C2α$^{cIII}$ mutant (Figure S4). These data indicate that

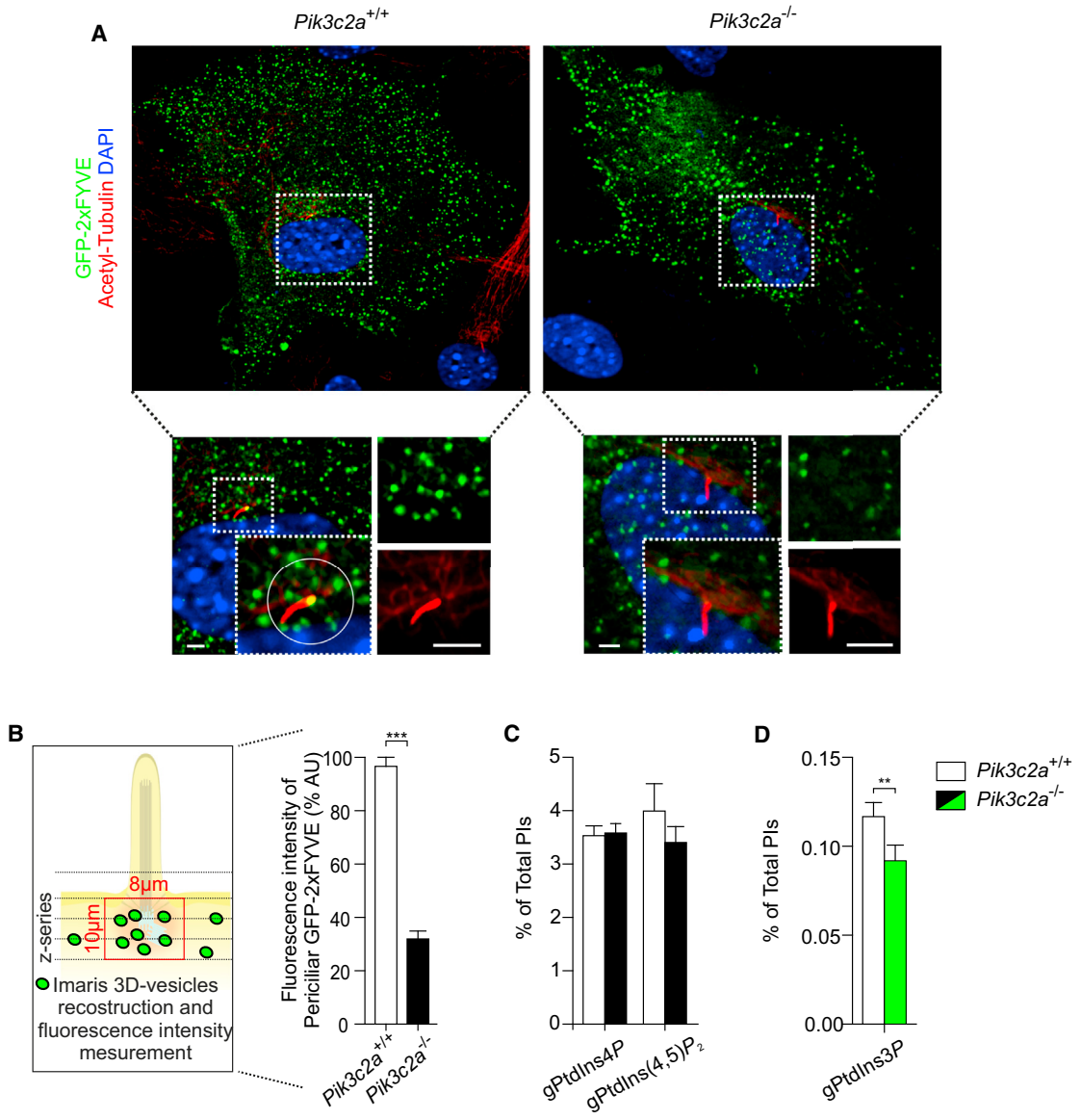


**Figure 2. PI3K-C2α Produces a Specific Pool of *PtdIns3P* around the Ciliary Base**

(A and B) Representative images (A) and quantification (B) of PtdIns3*P* at the ciliary base in wild-type and *Pik3c2a*$^{-/-}$ quiescent MEFs. *PtdIns3P* was detected with a specific 2x-GFP-FYVE probe and quantified by measuring the green fluorescent intensity around the ciliary base, in a region with a diameter of 8 um and depth of 10 um, as illustrated on the left (n = 25 cilia/genotype). Bar = 500 nm.

(C) HPLC analysis of phosphorylated phosphoinositides in either wild-type or *Pik3c2a*$^{-/-}$ serum-starved MEFs (three independent experiments).

(D) HPLC analysis of PtdIns3*P* showing a reduction in *Pik3c2a*$^{-/-}$ serum starved MEFs. Error bars indicate SEM.

PI3K-C2α-derived PtdIns3*P* is required to properly localize Rab11+ and TfR+ recycling vesicles to the pericentriolar area.

To assess the involvement of PI3K-C2α catalytic activity in triggering Rab11 activation, add-back experiments were performed by transfection of shRNA-resistant PI3K-C2α mutants in Sh1-3T3 cells. Although the wild-type enzyme restored Rab11 activity, a kinase-dead mutant was unable to revert Rab11 inactivation induced by PI3K-C2α downregulation (Figure 4B). Similar to rescue of Rab11 localization, expression of the PI3K-C2α$^{cIII}$ mutant was sufficient to fully restore Rab11 activity (Figure 4B). These results indicate that PI3K-C2α is required and sufficient for production of a pool of PtdIns3*P* critically needed for Rab11 localization and activation at the PRE.

## Loss of PI3K-C2α Impairs Rab8 Activation and Ciliogenesis

At the ciliary base, active Rab11 promotes a cascade of signaling events, including the activation of Rab8 and its localization along the ciliary axoneme, where it controls cilium elongation (Westlake et al., 2011). To test if Rab11 mislocalization and inactivation induced by the loss of PI3K-C2α affected Rab8 function, red fluorescent protein (RFP)-tagged Rab8 was transfected into

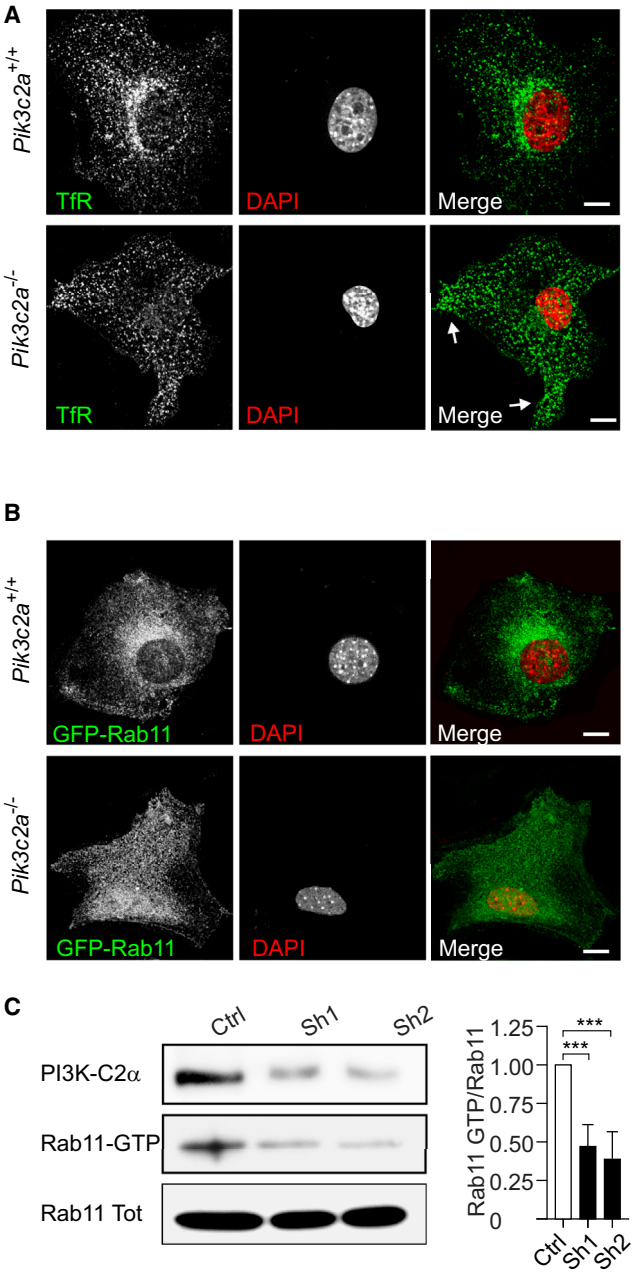


**Figure 3. PI3K-C2α Loss Impairs TfR/Rab11 Localization and Rab11 Activation**

(A) Immunofluorescence with antibody to transferrin receptor (TfR, green) in wild-type and *Pik3c2a*$^{-/-}$ MEFs showing that pericentriolar accumulation of this recycling endosome marker is lost in *Pik3c2a*$^{-/-}$ MEFs.

(B) Immunofluorescence of transfected Rab11-GFP (green) in wild-type and *Pik3c2a*$^{-/-}$ MEFs.

(C) Pull-down experiment showing the endogenous content of Rab11-GTP in NIH 3T3 cells infected with either a control sequence (empty-pGIPZ; Ctrl) or shRNAs downmodulating PI3K-C2α (Sh1 and Sh2). Quantification of four independent experiments is provided on the right. Error bars indicate SEM.

wild-type and *Pik3c2a*$^{-/-}$ MEFs to assess Rab8 localization 24 hr poststarvation, concomitantly with primary cilium formation. Although Rab8 localized along the ciliary axoneme in 70% of wild-type cilia, the percentage of Rab8-positive cilia was severely reduced in *Pik3c2a*$^{-/-}$ MEFs, thus confirming that PI3K-C2α promotes Rab8 function (Figures 5A and 5B).

Given the role of the Rab11/Rab8 axis in primary cilium formation (Knödler et al., 2010), the length of primary cilia was measured in wild-type, *Pik3c2a*$^{+/-}$, and *Pik3c2a*$^{-/-}$ MEFs. Ciliary length was significantly reduced in both *Pik3c2a*$^{+/-}$ and *Pik3c2a*$^{-/-}$ MEFs (Figures 5C and 5D), with a more pronounced shortening in *Pik3c2a*$^{-/-}$ (60%) compared to heterozygous MEFs (23%), indicating a dose-response effect. In agreement, *Pik3c2a* downmodulation in IMCD3 cells produced a 60% and 70% reduction in Rab8-positive cilia using Sh1 and Sh2, respectively (Figures S5A and S5B), accompanied by a 50% and 60% reduction in ciliary length (Figure S5C), further demonstrating that PI3K-C2α is involved in Rab11/Rab8-mediated cilium elongation.

Next, rescue of ciliary length was attempted by transfecting *Pik3c2a*$^{-/-}$ MEFs with PI3K-C2α and its mutant variants. Although the add back of a wild-type PI3K-C2α completely restored ciliary length, the kinase-dead mutant did not (Figure 5E), indicating a crucial role for PI3K-C2α catalytic activity in ciliary elongation. More importantly, reintroduction of the PI3K-C2α$^{cIII}$ mutant fully restored ciliary length (Figure 5E), indicating that the PI3K-C2α-dependent production of PtdIns3*P* is critical for this specific process. Furthermore, to test the involvement of Rab11 in this process, *Pik3c2a*$^{-/-}$ MEFs were transfected with either wild-type or constitutively active Rab11. The Q70L constitutively active Rab11 mutant was able to rescue ciliary length in *Pik3c2a*$^{-/-}$ MEFs, but neither the wild-type Rab11 nor the constitutively active mutant of a different Rab, Rab5 (Rab5$^{Q79L}$), produced any effect (Figure 5F).

## Abnormal Primary Cilia in Pik3c2a-Deficient Embryos

Given the well-established role of primary cilia in embryonic development (Goetz and Anderson, 2010), the embryonic-lethal phenotype induced by the loss of PI3K-C2α (Yoshioka et al., 2012) was re-evaluated in light of a cilium-related dysfunction. In line with a role in almost ubiquitous primary cilia, detection of the *lacZ* marker inserted into the mutant allele showed ubiquitous expression in *Pik3c2a*$^{+/-}$ embryos at all developmental stages analyzed (Figure S6A). Similarly to what previously reported (Yoshioka et al., 2012), homozygous inactivation of the *Pik3c2a* locus determined evident growth defects at embryonic day 8.5 (E8.5; Figure S6B) and lethality between E10.5 and E11.5 (Table S1). Consistent with ciliary defects observed in cultured cells, scanning electron microscopy, as well as immunofluorescence, revealed that cilia of the ventral node were frequently bent and swollen and with a 30% and 15% shorter shaft in *Pik3c2a*$^{-/-}$ and *Pik3c2a*$^{+/-}$ embryos, respectively (Figures 6A and 6B; Figures S6C and S6D). Thus, loss of PI3K-C2α is compatible with ciliogenesis but impairs primary cilium elongation in vivo.

## PI3K-C2α Is Required for Hh Pathway Activation

Analysis of *Pik3c2a*$^{-/-}$ embryos at E9.5/E10.5 showed that turning and cardiac tube looping were severely disturbed (Figures 6C and 6D; Figures S6E and S6F; Table S1). Furthermore, in situ hybridization failed to detect any expression of *Lefty1/2* and *Nodal* in *Pik3c2a*$^{-/-}$ embryos at the 1- to 5-somite stage, whereas these genes were correctly expressed in the ventral

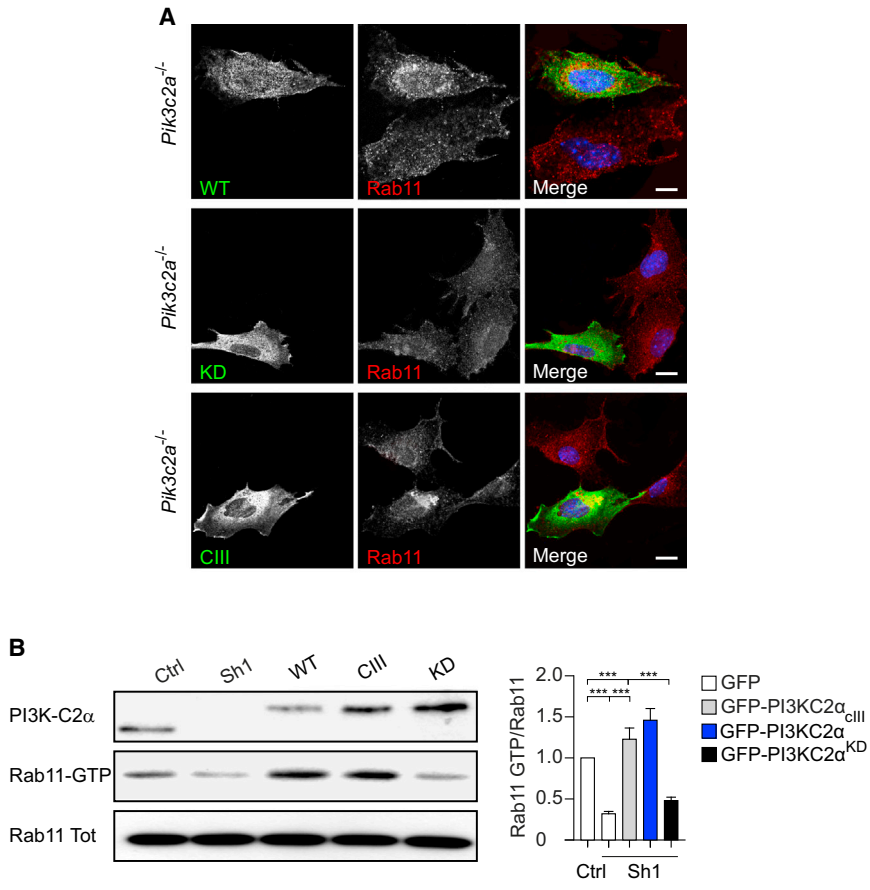


**Figure 4. PI3K-C2α-Dependent PtdIns3*P* Is Necessary for Rab11 Localization and Activity**

(A) Localization of endogenous Rab11 (red) in *Pik3c2a*$^{-/-}$ MEFs transfected with either wild-type (WT), kinase-inactive (KD), or class III mutated (CIII) PI3K-C2α-GFP (green) showing that only WT and CIII enzymes rescue Rab11 localization.

(B) Expression of WT, KD, or CIII PI3K-C2α-GFP in *Pik3c2a*-silenced NIH 3T3 cells to assess levels of active Rab11 (Rab11-GTP) by pull-down (left) and quantification (right, n = 6). Only PI3K-C2α forms able to produce PtdIns3*P* can rescue Rab11 activation. Error bars indicate SEM.

node and left lateral plate mesoderm of wild-type embryos at the same developmental stage (Figures 6E and 6F; Table S1), indicating that loss of PI3K-C2α impairs left-right patterning.

Embryonic lethality and laterality defects detected in *Pik3c2a*$^{-/-}$ embryos resembled the loss of the Hh signal transducer Smo, which depends on membrane traffic to the primary cilium for its function. In the node of 1- to 5-somite *Pik3c2a*$^{-/-}$ embryos, expression of the *Shh* mRNA was normally detected (Figure 7A). However, the Shh-dependent translocation of Smo to the shaft of ventral node cilia was severely reduced (Figure 7B; Figure S7A). Similarly, the number of Smo-positive cilia after Hh pathway stimulation was significantly decreased in *Pik3c2a*-silenced NIH 3T3 cells compared to control cells (Figure 7C; Figure S7B). A reduction of Smo ciliary localization was also obtained by transfecting in wild-type cells a dominant-negative (GFP-Rab11$^{S25N}$), but not a wild-type, Rab11 (Figure S7C). Conversely, transfection of the constitutively active mutant of Rab11 (GFP-Rab11$^{Q70L}$) (Figures 7D and 7E), as well as the Rab11-activating PI3K-C2α$^{cIII}$ mutant (Figure 7E), normalized Smo ciliary localization upon Hh-pathway stimulation in PI3K-C2α-deficient cells, demonstrating that the PI3K-C2α/Rab11 axis is required for efficient ciliary translocation of Smo.

This suggested that the lack of PI3K-C2α impairs one of the earliest events in Hh signaling, potentially blocking downstream signaling events in the Hh pathway in vivo. In agreement, loss of PI3K-C2α was found to alter the processing of the Gli3 transcription factor, which in 1- to 5-somite *Pik3c2a*$^{-/-}$ embryos was present in a significantly higher amount as a repressor (R) short form than as a full-length transcriptional activator form (Figure 7F; Figure S7D). Furthermore, transcripts for Shh downstream targets *Ptch1* and *Gli1* were reduced by 53% and 57% in *Pik3c2a*$^{-/-}$ 1- to 5-somite embryos compared to wild-type controls, whereas the Hh unrelated gene *FGF8* was equally expressed in both genotypes (Figure 7G). In further agreement with a reduced Hh signaling, Shh-mediated dorsoventral patterning of the neural tube was severely altered in E10.5 *Pik3c2a*$^{-/-}$ embryos. In particular, expression of Shh-dependent markers of ventral neural cell types, such as Shh, FoxA2, and Nkx2.2, was absent, whereas expression of the Shh-inhibited Pax6 expanded to ventral cells (Figure S7E).

In mutant MEFs, analysis of Shh-induced target gene expression accordingly revealed that the upregulation of *Ptch1* and *Gli1* after 24 hr stimulation with 100 nM Shh was significantly lower than that of wild-type controls (Figure 7H). A significant reduction in Shh-mediated target gene transcription was also confirmed in Sh1-3T3 cells (Figure 7I). This experimental system was next used to test the role of PI3K-C2α catalytic activity and of Rab11 in Shh pathway activation. Expression of an shRNA-resistant PI3K-C2α$^{cIII}$ mutant showed a significant rescue of both *Gli1* and *Ptch1* Shh-mediated transcriptional upregulation, indicating that PtdIns3*P* produced by PI3K-C2α is critically required for Shh signaling pathway activation. Similarly, a constitutively active Rab11$^{Q70L}$ mutant, but not a wild-type Rab11, was able to fully restore sensitivity to Shh (Figure 7I). Collectively, these results establish a critical requirement for PI3K-C2α-mediated production of PtdIns3*P* for the organization of the perinuclear recycling compartment and for Shh signaling, both in vivo and in cultured cells.

## DISCUSSION

Four distinct PI3Ks (the three class II α, β, γ enzymes and the class III PI3K) can in principle generate PtdIns3*P* in vivo (Vanhaesebroeck et al., 2010), but whether each of these enzymes contributes only to a specific pool of PtdIns3*P* with distinct

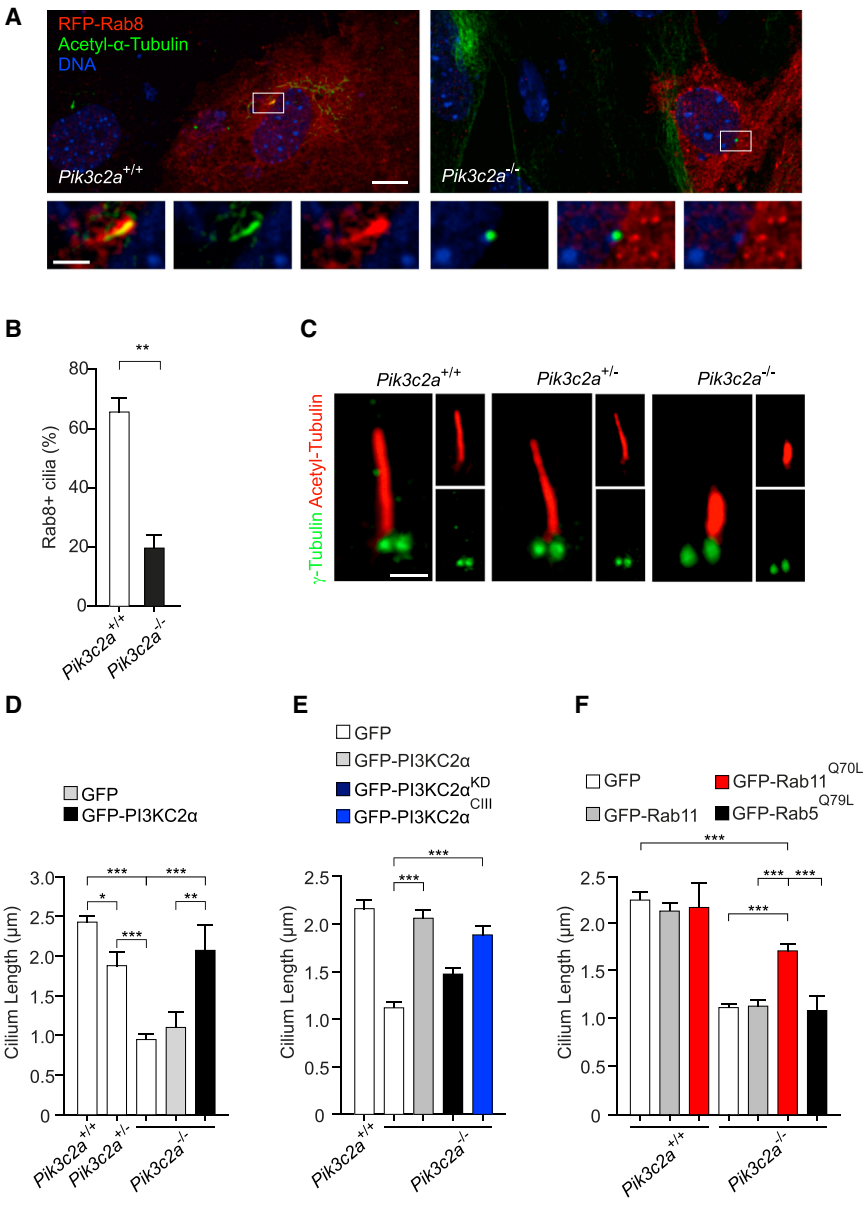


**Figure 5. Loss of PI3K-C2α Impairs Ciliary Localization of Rab8 and Cilium Elongation**

(A) Immunofluorescence of RFP-Rab8 (red) and acetylated α-tubulin (green) in 24-hr-starved MEFs. Rab8 localizes at the cilium during cilia formation in wild-type MEFs, whereas it is absent from ciliary axoneme in *Pik3c2a*$^{-/-}$ MEFs. Bar = 2 μm.

(B) Quantification of Rab8 positive cilia in wild-type and *Pik3c2a*$^{-/-}$ MEFs. Wild-type and *Pik3c2a*$^{-/-}$ MEFs were transfected with RFP-Rab8. Among RFP-positive cells, those showing a cilium were scored for the presence of Rab8 and the percentage of positive cilia over the total number of cilia was calculated. At least 30 cilia per genotype were quantified in three different experiments.

(C) Immunofluorescence with antibody to γ-tubulin (green) and acetylated α-tubulin (red) showing abnormal cilium length and shape in *Pik3c2a*$^{-/-}$ MEFs. Bar = 1 μm.

(D) Analysis of cilium length in wild-type, *Pik3c2a*$^{+/-}$, and *Pik3c2a*$^{-/-}$ MEFs (n = 200 cilia in three independent experiments). *Pik3c2a*$^{-/-}$ MEFs were transfected with either GFP or GFP-tagged PI3K-C2α plasmids to test the rescue of ciliary length (n = 60 cilia).

(E) Analysis of primary cilium length in *Pik3c2a*$^{-/-}$ MEFs transfected with either wild-type or mutant forms of GFP-tagged PI3K-C2α (n = 100 cilia in three independent experiments). Transfection with a PI3K-C2α mutant that can only generate PtdIns3*P* (PI3K-C2α$^{CIII}$) fully restores ciliary length, whereas the kinase-inactive (PI3K-C2α$^{KD}$) mutant only partially rescues the cilium length defect (n = 200 cilia in three independent experiments).

(F) Analysis of primary cilium length in wild-type and *Pik3c2a*$^{-/-}$ MEFs transfected with either wild-type or constitutively active (Q70L) Rab11 (n = 100 cilia in three independent experiments). Wild-type Rab11 and constitutively active Rab5 (Q79L) are used as negative controls. Error bars indicate SEM.

intracellular function has long remained obscure. Our results help to elucidate the localization and role of a distinct PtdIns3*P* pool by demonstrating that PtdIns3*P* selectively produced by PI3K-C2α is concentrated at the PRE and promotes the correct pericentriolar localization of Rab11+ vesicles as well as the activation of Rab11. This triggers the Rab8-dependent pathway as well as the translocation of Smo to the primary cilium, a process involved in the activation of Shh signal transduction cascade.

Our experiments with fluorescently labeled PtdIns3*P* probes and anti-PtdIns3*P* antibodies as well as HPLC analysis showed that in the absence of PI3K-C2α, a small, highly localized PtdIns3*P* pool was missing. The finding that loss of PI3K-C2α causes reduced levels of PtdIns3*P* matches what has been reported using an independently generated PI3K-C2α-deficient mouse strain (Yoshioka et al., 2012) as well as silenced cells (Falasca et al., 2007). The small but significant reduction in PtdIns3*P* detected in the absence of PI3K-C2α was found to reflect a specific enrichment of this enzyme at the PRE. This observation links PI3K-C2α to the recycling compartment and suggests that this enzyme plays a specific function at this subcellular location. The finding that PI3K-C2α-derived PtdIns3*P* controls the Rab11/Rab8 axis further supports this hypothesis. Our results thus indicate that PI3K-C2α has multiple functions at different subcellular locations and that its role at the PRE is distinct from that played, for example, at the plasma membrane (Posor et al., 2013). At the cell surface, PI3K-C2α is located in clathrin-coated pits, where it specifically generates PtdIns(3,4)$P_2$. This lipid then favors Snx9 recruitment, followed by Dynamin association and cleavage of the membrane neck required to form a free vesicle. As a consequence, loss of PI3K-C2α causes a severe impairment of clathrin-dependent endocytosis. A PI3K-C2α mutant (PI3K-C2α CIII) that can only generate PtdIns3*P* does not rescue this defect (Posor et al., 2013) but does, unexpectedly, fully restore Rab11 localization and activation as well as primary

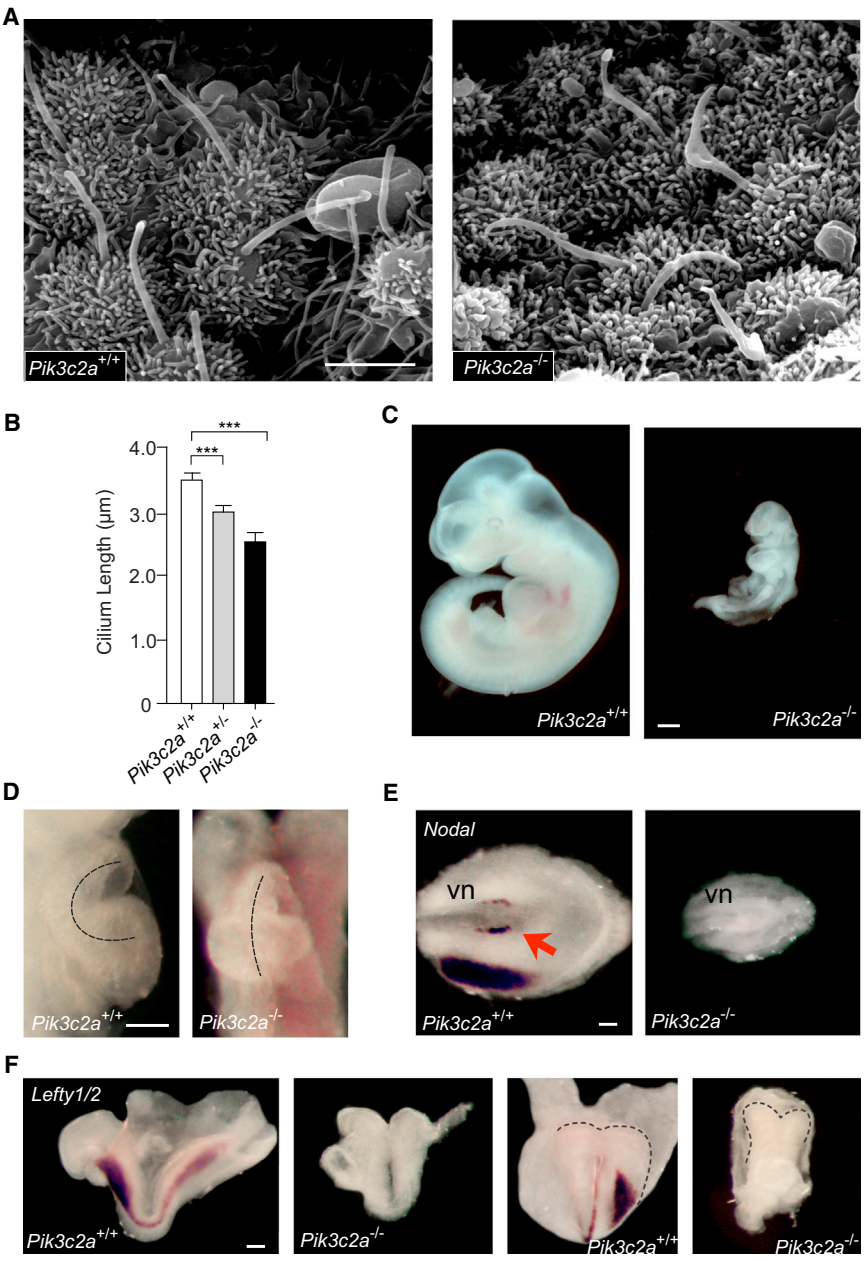


**Figure 6. Phenotypes of *Pik3c2a* Mutant Embryos**

(A) SEM analysis of cilia morphology in the ventral node of wild-type and *Pik3c2a*$^{-/-}$ embryos at the presomitic stage. Bar = 3 μm.

(B) Quantification of cilium length from SEM images (n = 30 cilia/genotype).

(C) E10.5 *Pik3c2a*$^{-/-}$ embryos fail to complete axial rotation and turning. Bar = 500 μm.

(D) Defective cardiac looping in *Pik3c2a*-null embryos at E10.5. Approximately 60% of examined embryos showed this anomaly (n = 41). Bar = 100 μm.

(E) Detection of *Nodal* by in situ hybridization at the ventral node and lateral-plate mesoderm of wild-type and *Pik3c2a*$^{-/-}$ embryos at the 1- to 5-somite stage (n = 6). Bar = 200 μM. vn, ventral node; arrow points to increased *Nodal* expression in the left side of the wild-type node.

(F) Expression of *Lefty1/2* in wild-type and *Pik3c2a*$^{-/-}$ embryos at the 1- to 5-somite stage; lateral and frontal views. Bar = 200 μM. n = 6. Error bars indicate SEM.

cilium-dependent Shh signaling. This demonstrates that the activity of PI3K-C2α at the PRE is in principle independent from the endocytic defect. Together with recent work from Posor et al. (2013), our findings suggest that the substrate specificity of PI3K-C2α in vivo may be determined in a compartment-specific manner, e.g., by substrate availability. According to this model, PtdIns serves as a preferential PI3K-C2α substrate at recycling endosomes, which likely contain little PtdIns*P*4 (Krauss and Haucke, 2007), in contrast to the plasma membrane (Hammond et al., 2012). However, we currently cannot rule out the possibility that PI3K-C2α produces a pool of PtdIns(3,4)$P_2$ that is then rapidly converted into PtdIns3*P* by 4P phosphatases such as INPP4B (Gewinner et al., 2009). The inability to specifically target such phosphatases to the PRE prevented us from examining this possible mechanism of action in detail.

Remarkably, the pool of PtdIns3*P* generated by PI3K-C2α and associated with the PRE was found to specifically control Rab11 localization and activity, whereas it did not affect localization of the endosomal marker Rab5. PI3K-C2α and Rab11 were found to colocalize but could not be coimmunoprecipitated, suggesting that PI3K-C2α does not directly associate with Rab11. The loss of PI3K-C2α-dependent PtdIns3*P* generation might thus impair Rab11 activation through other, possibly indirect mechanisms that require further investigation. Nonetheless, our results clearly point to an unexpected epistatic interaction placing PI3K-C2α-dependent PtdIns3*P* production upstream of Rab11 activation.

In the endosomal compartment, class III PI3K-dependent PtdIns3*P* synthesis leads to late endosome maturation (Backer, 2008; Stein et al., 2003), whereas our results suggest that PI3K-C2α-dependent PtdIns3*P* is involved in endosomal recycling. Consistently, the *Drosophila* homolog of class II PI3Ks, Pi3k68D, produces PtdIns3*P* required for the exit of vesicles from the endocytic compartment, sorting toward the plasma membrane, and cell protrusion formation (Jean et al., 2012; Velichkova et al., 2010). Furthermore, a previous report indicates that the loss of PI3K-C2α in endothelial cells leads to defective delivery of VE-cadherin to cell junctions, thereby causing impaired assembly of endothelial junctions and disrupted vessel integrity in *Pik3c2a* mouse mutants (Yoshioka et al., 2012). Considering the established role of Rab11 in the control of cadherin traffic (Lock and Stow, 2005), and in light of the results we present here, this

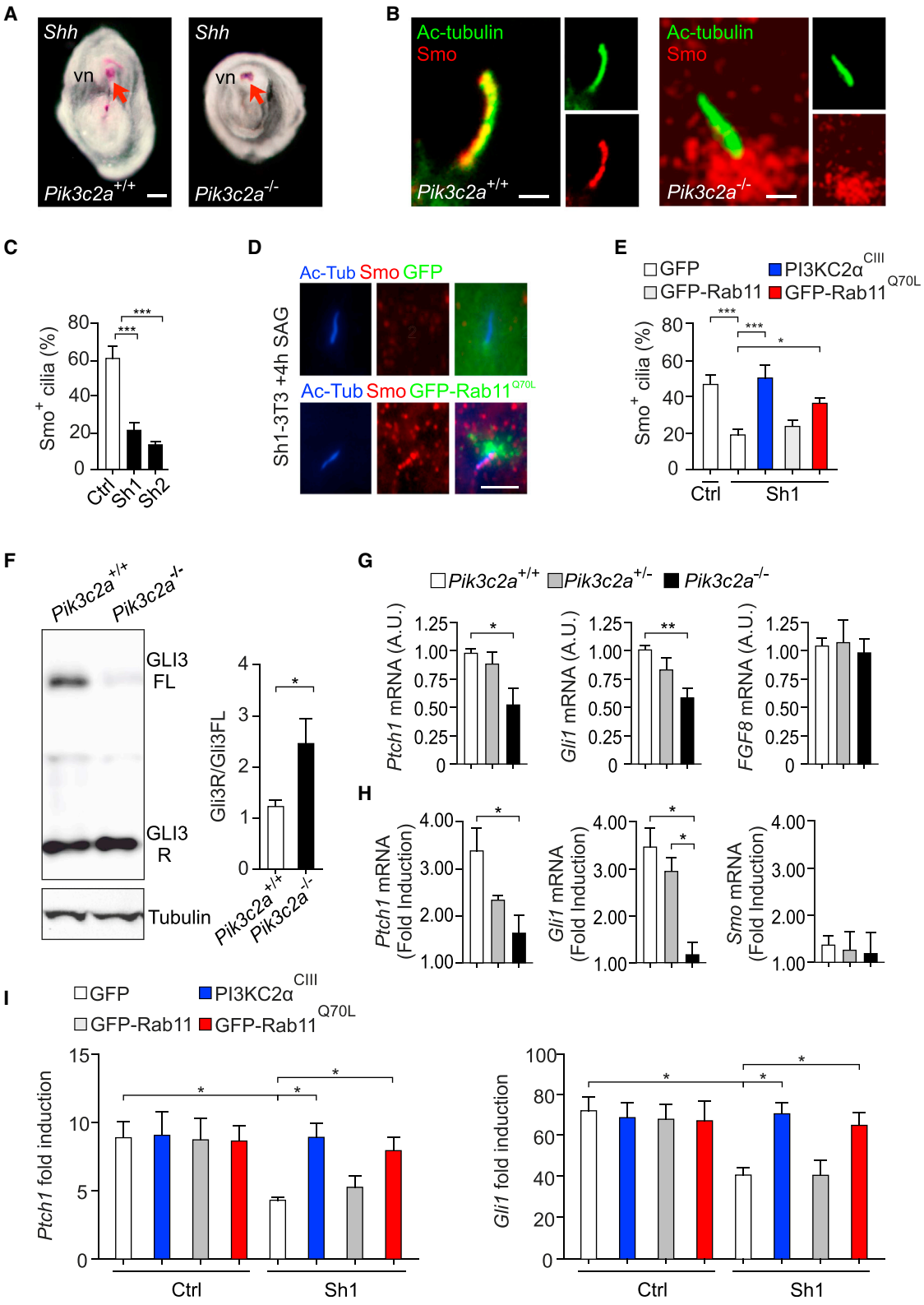


**Figure 7. Defective Hh Signaling in *Pik3c2a* Mutant MEFs and Embryos**

(A) Expression of *Shh* in the ventral node area (arrows) by in situ hybridization; ventral view. vn, ventral node.

(B) Immunofluorescence analysis of Smoothened (Smo, red) localization at the nodal cilia (acetylated α-tubulin, green) of presomite wild-type and *Pik3c2a*$^{-/-}$ embryos (n = 5). Bar = 500 nm.

*(legend continued on next page)*

phenotype is conceivably linked to the loss of Rab11 activity, a possibility that needs further assessment. On the other hand, our data clearly show that the epistatic interaction between PI3K-C2α-dependent PtdIns3*P* production and Rab11 activation at the PRE is required at earlier developmental stages and is critical for Rab8 and Smo translocation to the plasma membrane and, ultimately, for primary cilium signaling functions.

In line with this view, the phenotype of *Pik3c2a*-null embryos indicates that PI3K-C2α is a major player in cargo delivery to the primary cilium. This is particularly evident at the ventral node, where Smo did not reach the ciliary shaft. Our results with the PI3K-C2α CIII and Rab11Q70L mutants restoring the response to Shh stimulation demonstrate a critical role for Rab11/PRE-dependent traffic in Smo translocation to the cilium. Although part of the ciliary Smo can derive from the endocytic recycling compartment (Kim et al., 2010), another source is provided by lateral transport on the plasma membrane (Milenkovic et al., 2009). Given the Rab11 delocalization/deactivation induced by the loss of PI3K-C2α-derived PtdIns3*P*, it is possible that the trafficking dysfunction affects the pool of Smo at the plasma membrane as well. In line with this hypothesis, Shh signaling was fully restored in PI3K-C2α-deficient cells by either the PI3K-C2α CIII mutant or the constitutively active form of Rab11.

In agreement with the profound effect on Smo localization and Shh signaling, embryos lacking PI3K-C2α showed a series of developmental abnormalities typically detected in the loss of Hh signaling. Although a previous report suggested that the loss of PI3K-C2α causes lethality because of abnormal endothelial cell function (Yoshioka et al., 2012), several of these phenotypes appeared earlier than vasculogenesis. Phenotypes detected in *Pik3c2a*$^{-/-}$ embryos do not match those detected in conditions where the primary cilium is absent that show, for example, bilateral expression of *Nodal* and *Lefty* and consequent randomization of situs (Huangfu et al., 2003; Murcia et al., 2000; Nonaka et al., 1998) as well as defective cleavage of Gli3 (Huangfu and Anderson, 2005). Consistent with this observation, the loss of PI3K-C2α did not abolish cilia, which are yet shorter and swollen, likely as a consequence of defective trafficking of ciliary components. On the contrary, phenotypes of *Pik3c2a*$^{-/-}$ embryos largely overlapped with those of embryos lacking Smo or showing defective Hh signal transduction activation. These embryos, for example, show smaller size, no turning, no cardiac looping, complete loss of expression of *Nodal* and *Lefty*, and increased Gli3 cleavage (Huangfu and Anderson, 2005; Zhang et al., 2001). These observations suggest that loss of PI3K-C2α does not affect Gli3 cleavage but blocks PtdIns3P as well as Rab11-dependent ciliary targeting of Smo, thus impairing Hh signal activation.

These findings place PI3K-C2α in an epistatic interaction with the Hh signaling machinery and explain a large set of the developmental abnormalities found in *Pik3c2a*$^{-/-}$ embryos. Our data cannot rule out that the multifaceted functions of PI3K-C2α at the plasma membrane (Posor et al., 2013) and at adherens junctions (Yoshioka et al., 2012) contribute to the in vivo phenotype. Nonetheless, we provide genetic evidence that PI3K-C2α crucially regulates a PtdIns3*P*-dependent membrane traffic at the PRE that acts upstream of Rab11 localization/activation and promotes Smo ciliary targeting and Shh signaling.

## EXPERIMENTAL PROCEDURES

### Animal Models

A *lacZ* (bacterial β-galactosidase)-*neoR* cassette was inserted in-frame with the ATG start codon of *Pik3c2a* via bacterial recombination. Constructs were electroporated in embryonic stem cells and chimeras obtained by standard procedures. Mice were backcrossed for eight generations in the C57Bl/6J; wild-type littermates from heterozygous crosses were used as controls. The experiments involving mutant and wild-type mice were carried out according to European Union (86/609/CEE, CE Off J n°L358, 18 December 1986) and institutional animal welfare guidelines and legislation and approved by the local ethics committee.

### MEF Derivation, Culture, and Treatments

Primary cultures of MEFs were generated from individual E11.5 littermates by trypsinization of eviscerated embryonic bodies and expanded and maintained in Dulbecco's modified Eagle's medium supplemented with 10% fetal bovine serum. Early-passage cells (less than four passages) were used for analysis. Starvation and cilium assembly were achieved by 72 hr of serum deprivation. MEFs at 80% confluency were transfected on coverslips in 24-well plates with 0.5 μg of plasmid DNA using the Effectene transfection reagent (QIAGEN). For Shh experiments, MEFs and NIH 3T3 cells were plated at near-confluent densities and serum starved for 48 hr prior to treatment to allow ciliation. Rm-Shh-N (R&D Systems) stimulation lasted 24 hr. Other procedures are reported in Supplemental Experimental Procedures.

(C) Quantification of Smo positive cilia in control and *Pik3c2a*-silenced NIH 3T3 cells shown in Figure S7B. Cells were starved for 48 hr to allow ciliation and then stimulated with SAG 100 nM for 4 hr. Provided is the mean percentage of Smo+ cilia per field. At least 80 cilia per genotype have been counted in three independent experiments.

(D) Representative images showing Smo (red) accumulation in cilia (acetyl-tubulin, blue) upon stimulation with the Hedgehog (Hh) pathway activator SAG (4 hr, 100 nM) in *Pik3c2a*-silenced NIH 3T3 cells after transfection with either a control plasmid (GFP, green) or the constitutively active mutant of Rab11 (GFP-Rab11$^{Q70L}$, green).

(E) Quantification of Smo-positive cilia in control and *Pik3c2a*-silenced NIH 3T3 cells (Sh1-3T3) transfected with different plasmids: GFP (shown in D, upper panels), GFP- PI3K-C2α$^{cIII}$, GFP-Rab11, and GFP-Rab11$^{Q70L}$ (shown in D, lower panels). At least 90 GFP-positive cells per genotype have been counted.

(F) Representative western blot and quantification of Gli3 R/ Gli3 full length in wild-type and *Pik3c2a*$^{-/-}$ embryos (n = 5).

(G) Gene expression in wild-type, *Pik3c2a*$^{+/-}$, and *Pik3c2a*$^{-/-}$ 1- to 5-somite-stage embryos, assessed by real-time quantitative PCR (qPCR) (n = 9). Levels of Hh targets *Ptch1* and *Gli1* are decreased in the absence of PI3K-C2α, whereas the Hh-independent gene *FGF8* is unchanged in the three genotypes.

(H) Quantification of Shh-induced responses in wild-type, *Pik3c2a*$^{+/-}$, and *Pik3c2a*$^{-/-}$ MEFs. Real-time qPCR measurement of *Ptch1, Gli1*, and *Smo* mRNA in cells stimulated with 100 nM Shh for 24 hr was divided for values measured in untreated cells to calculate the fold induction. Provided is the mean of fold induction values obtained in four independent experiments.

(I) qPCR measurement of *Ptch1* and *Gli1* upregulation after Shh treatment. NIH 3T3 cells were infected with either a control vector or Sh1 shRNA to silence *Pik3c2a*. Transfection of either PI3K-C2α$^{cIII}$ or Rab11$^{Q70L}$ rescues Shh response defects detectable in Sh1-3T3 cells transfected with a control vector (GFP), whereas transfection of wild-type Rab11 was ineffective (six independent experiments). Error bars indicate SEM.

### Materials

Plasmids, antibodies, and other reagents are listed in Supplemental Experimental Procedures.

### Pik3c2a Silencing

Plasmids containing shRNA sequences (arrest GIPZ lentiviral shRNAmir) against Mm *Pik3c2a* were purchased from Thermo Scientific and used to generate lentiviral particles to stably infect NIH 3T3 and IMCD3 cells as described in Supplemental Experimental Procedures. The Sh1 (V2LMM_73461) target sequence was 5′-GGCAAGATATGTTAGCTTT-3′, and the Sh2 (V2LMM_66190) target sequence was 5′-CAAAGTTTCTTTAACTCT-3′. Cells at early passages after infection (second to third) were used for experiments. Sh1-resistant wild-type, kinase-inactive (KD), and class III (cIII) PI3KC2α were generated by creating three silent mutations in the human pEGFP–PI3KC2a with the QuikChange site-directed mutagenesis kit (Stratagene) using the following primer: 5′-GTTTAAGGTTGGTGAAGATCTTCGCCAGGACATGTTAG CTTTACAGA-3′ and transfected using the Effectene transfection reagent.

### Generation of the Rab11 Binding Domain Probe

The C-terminal portion of the Rab11 effector FIP3 (Rab11 binding domain) was cloned in pGex 4T2 vector. Recombinant protein was produced in bacteria (4 hr induction at room temperature), purified (elution 10 mM glutathione, PBS), dialyzed, frozen in liquid nitrogen, and stocked (50% glycerol in Tris-HCl 50 mM 5 mM MgCl2, 100 mM NaCl) at −80°C.

### Pull-Down

Cells were washed in ice-cold PBS and lysed in 1 ml of MLB buffer (25 mM HEPES [pH 7.5], 150 mM NaCl, 1% Igepal CA-630, 10% glycerol, 25 mM NAF, 10 mM MgCl2, 1 mM EDTA, 1mM sodium orthovanadate, and protease inhibitor cocktail). Supernatant was collected after 15 min centrifugation at 13,000 rpm. A total of 500 μg of protein extract was incubated with 30 μg of recombinant protein coupled with glutathione S-transferase agarose. The reaction mixture was gently rocked for 1 hr at 4°C. Beads were washed four times with lysis buffer. Samples were resuspended in Laemmli buffer for SDS-PAGE and immunoblot analysis. Endogenous content of total Rab11 in cell lysates was measured by loading 50 μg of total extracts in a different gel followed by immunoblot and used to normalize measurements of active Rab11. For quantification analysis, pictures were taken ensuring that intensity was within the linear range and the Quantity One 1-D analysis software (Bio-Rad) was used.

### Statistical Analyses

Values are reported as the mean ± SEM. Statistical significance was calculated with one-way ANOVA and Bonferroni post hoc tests. One, two, and three asterisks in all the figures indicate significance with a p value <0.05, <0.01, and <0.001, respectively. All the analyses were performed with the software PRISM5 (GraphPad Software).

All other procedures are reported in Supplemental Experimental Procedures.

## SUPPLEMENTAL INFORMATION

Supplemental Information includes Supplemental Experimental Procedures, seven figures, and one table and can be found with this article online at http://dx.doi.org/10.1016/j.devcel.2014.01.022.

## ACKNOWLEDGMENTS

We thank B. Franco (Tigem, Naples, Italy), S. Schurmanns (University of Brussels, Belgium), R. Rohatgi and C.E. Hughes (Stanford University, USA), F. Luzzati (University of Torino, Italy), and L. Lanzetti (IRCC, Candiolo, Italy) for helpful discussion and reagents and all the members of E.H.'s laboratory. This work was supported by grants from AIRC, Italy (to E.H.), the European Union FP-VI EuGeneHeart (to E.H.), Regione Piemonte, Italy (to E.H.), Leducq Foundation, France (to E.H.), Progetto Ateneo Compagnia San Paolo, Italy (to E.H.), Telethon Foundation, Italy (to A.B. and G.R.M.), and the German Funding Agency DFG (SFB740/C08 and SFB958/A07, to V.H.). The CMMI is supported by the European Regional Development Fund and the Walloon Region.

Received: August 14, 2012
Revised: October 15, 2013
Accepted: January 23, 2014
Published: March 31, 2014

## REFERENCES

Backer, J.M. (2008). The regulation and function of class III PI3Ks: novel roles for Vps34. Biochem. J. *410*, 1–17.

Bielas, S.L., Silhavy, J.L., Brancati, F., Kisseleva, M.V., Al-Gazali, L., Sztriha, L., Bayoumi, R.A., Zaki, M.S., Abdel-Aleem, A., Rosti, R.O., et al. (2009). Mutations in INPP5E, encoding inositol polyphosphate-5-phosphatase E, link phosphatidyl inositol signaling to the ciliopathies. Nat. Genet. *41*, 1032–1036.

Christoforidis, S., Miaczynska, M., Ashman, K., Wilm, M., Zhao, L., Yip, S.C., Waterfield, M.D., Backer, J.M., and Zerial, M. (1999). Phosphatidylinositol-3-OH kinases are Rab5 effectors. Nat. Cell Biol. *1*, 249–252.

Corbit, K.C., Aanstad, P., Singla, V., Norman, A.R., Stainier, D.Y., and Reiter, J.F. (2005). Vertebrate Smoothened functions at the primary cilium. Nature *437*, 1018–1021.

Das, A., and Guo, W. (2011). Rabs and the exocyst in ciliogenesis, tubulogenesis and beyond. Trends Cell Biol. *21*, 383–386.

Devereaux, K., Dall'Armi, C., Alcazar-Roman, A., Ogasawara, Y., Zhou, X., Wang, F., Yamamoto, A., De Camilli, P., and Di Paolo, G. (2013). Regulation of mammalian autophagy by class II and III PI 3-kinases through PI3P synthesis. PLoS ONE *8*, e76405.

Di Paolo, G., and De Camilli, P. (2006). Phosphoinositides in cell regulation and membrane dynamics. Nature *443*, 651–657.

Eathiraj, S., Mishra, A., Prekeris, R., and Lambright, D.G. (2006). Structural basis for Rab11-mediated recruitment of FIP3 to recycling endosomes. J. Mol. Biol. *364*, 121–135.

Falasca, M., and Maffucci, T. (2012). Regulation and cellular functions of class II phosphoinositide 3-kinases. Biochem. J. *443*, 587–601.

Falasca, M., Hughes, W.E., Dominguez, V., Sala, G., Fostira, F., Fang, M.Q., Cazzolli, R., Shepherd, P.R., James, D.E., and Maffucci, T. (2007). The role of phosphoinositide 3-kinase C2alpha in insulin signaling. J. Biol. Chem. *282*, 28226–28236.

Feng, S., Knödler, A., Ren, J., Zhang, J., Zhang, X., Hong, Y., Huang, S., Peränen, J., and Guo, W. (2012). A Rab8 guanine nucleotide exchange factor-effector interaction network regulates primary ciliogenesis. J. Biol. Chem. *287*, 15602–15609.

Follit, J.A., Tuft, R.A., Fogarty, K.E., and Pazour, G.J. (2006). The intraflagellar transport protein IFT20 is associated with the Golgi complex and is required for cilia assembly. Mol. Biol. Cell *17*, 3781–3792.

Gewinner, C., Wang, Z.C., Richardson, A., Teruya-Feldstein, J., Etemadmoghadam, D., Bowtell, D., Barretina, J., Lin, W.M., Rameh, L., Salmena, L., et al. (2009). Evidence that inositol polyphosphate 4-phosphatase type II is a tumor suppressor that inhibits PI3K signaling. Cancer Cell *16*, 115–125.

Ghigo, A., Damilano, F., Braccini, L., and Hirsch, E. (2010). PI3K inhibition in inflammation: Toward tailored therapies for specific diseases. Bioessays *32*, 185–196.

Goetz, S.C., and Anderson, K.V. (2010). The primary cilium: a signalling centre during vertebrate development. Nat. Rev. Genet. *11*, 331–344.

Grant, B.D., and Donaldson, J.G. (2009). Pathways and mechanisms of endocytic recycling. Nat. Rev. Mol. Cell Biol. *10*, 597–608.

Hammond, G.R., Fischer, M.J., Anderson, K.E., Holdich, J., Koteci, A., Balla, T., and Irvine, R.F. (2012). PI4P and PI(4,5)P2 are essential but independent lipid determinants of membrane identity. Science *337*, 727–730.

Hsiao, Y.C., Tuz, K., and Ferland, R.J. (2012). Trafficking in and to the primary cilium. Cilia *1*, 4.

Huangfu, D., Liu, A., Rakeman, A.S., Murcia, N.S., Niswander, L., and Anderson, K.V. (2003). Hedgehog signalling in the mouse requires intraflagellar transport proteins. Nature *426*, 83–87.

Huangfu, D., and Anderson, K.V. (2005). Cilia and Hedgehog responsiveness in the mouse. Proc. Natl. Acad. Sci. USA *102*, 11325–11330.

Jacoby, M., Cox, J.J., Gayral, S., Hampshire, D.J., Ayub, M., Blockmans, M., Pernot, E., Kisseleva, M.V., Compère, P., Schiffmann, S.N., et al. (2009). INPP5E mutations cause primary cilium signaling defects, ciliary instability and ciliopathies in human and mouse. Nat. Genet. *41*, 1027–1031.

Jean, S., and Kiger, A.A. (2012). Coordination between RAB GTPase and phosphoinositide regulation and functions. Nat. Rev. Mol. Cell Biol. *13*, 463–470.

Jean, S., Cox, S., Schmidt, E.J., Robinson, F.L., and Kiger, A. (2012). Sbf/MTMR13 coordinates PI(3)P and Rab21 regulation in endocytic control of cellular remodeling. Mol. Biol. Cell *23*, 2723–2740.

Keady, B.T., Samtani, R., Tobita, K., Tsuchya, M., San Agustin, J.T., Follit, J.A., Jonassen, J.A., Subramanian, R., Lo, C.W., and Pazour, G.J. (2012). IFT25 links the signal-dependent movement of Hedgehog components to intraflagellar transport. Dev. Cell *22*, 940–951.

Kim, J., Lee, J.E., Heynen-Genel, S., Suyama, E., Ono, K., Lee, K., Ideker, T., Aza-Blanc, P., and Gleeson, J.G. (2010). Functional genomic screen for modulators of ciliogenesis and cilium length. Nature *464*, 1048–1051.

Knödler, A., Feng, S., Zhang, J., Zhang, X., Das, A., Peränen, J., and Guo, W. (2010). Coordination of Rab8 and Rab11 in primary ciliogenesis. Proc. Natl. Acad. Sci. USA *107*, 6346–6351.

Krauss, M., and Haucke, V. (2007). Phosphoinositide-metabolizing enzymes at the interface between membrane traffic and cell signalling. EMBO Rep. *8*, 241–246.

Liem, K.F., Jr., Ashe, A., He, M., Satir, P., Moran, J., Beier, D., Wicking, C., and Anderson, K.V. (2012). The IFT-A complex regulates Shh signaling through cilia structure and membrane protein trafficking. J. Cell Biol. *197*, 789–800.

Lock, J.G., and Stow, J.L. (2005). Rab11 in recycling endosomes regulates the sorting and basolateral transport of E-cadherin. Mol. Biol. Cell *16*, 1744–1755.

Maffucci, T., Brancaccio, A., Piccolo, E., Stein, R.C., and Falasca, M. (2003). Insulin induces phosphatidylinositol-3-phosphate formation through TC10 activation. EMBO J. *22*, 4178–4189.

Milenkovic, L., Scott, M.P., and Rohatgi, R. (2009). Lateral transport of Smoothened from the plasma membrane to the membrane of the cilium. J. Cell Biol. *187*, 365–374.

Murcia, N.S., Richards, W.G., Yoder, B.K., Mucenski, M.L., Dunlap, J.R., and Woychik, R.P. (2000). The Oak Ridge Polycystic Kidney (orpk) disease gene is required for left-right axis determination. Development *127*, 2347–2355.

Nachury, M.V., Loktev, A.V., Zhang, Q., Westlake, C.J., Peränen, J., Merdes, A., Slusarski, D.C., Scheller, R.H., Bazan, J.F., Sheffield, V.C., and Jackson, P.K. (2007). A core complex of BBS proteins cooperates with the GTPase Rab8 to promote ciliary membrane biogenesis. Cell *129*, 1201–1213.

Nonaka, S., Tanaka, Y., Okada, Y., Takeda, S., Harada, A., Kanai, Y., Kido, M., and Hirokawa, N. (1998). Randomization of left-right asymmetry due to loss of nodal cilia generating leftward flow of extraembryonic fluid in mice lacking KIF3B motor protein. Cell *95*, 829–837.

Ocbina, P.J., Eggenschwiler, J.T., Moskowitz, I., and Anderson, K.V. (2011). Complex interactions between genes controlling trafficking in primary cilia. Nat. Genet. *43*, 547–553.

Pedersen, L.B., and Rosenbaum, J.L. (2008). Intraflagellar transport (IFT) role in ciliary assembly, resorption and signalling. Curr. Top. Dev. Biol. *85*, 23–61.

Posor, Y., Eichhorn-Gruenig, M., Puchkov, D., Schöneberg, J., Ullrich, A., Lampe, A., Müller, R., Zarbakhsh, S., Gulluni, F., Hirsch, E., et al. (2013). Spatiotemporal control of endocytosis by phosphatidylinositol-3,4-bisphosphate. Nature *499*, 233–237.

Shin, H.W., Hayashi, M., Christoforidis, S., Lacas-Gervais, S., Hoepfner, S., Wenk, M.R., Modregger, J., Uttenweiler-Joseph, S., Wilm, M., Nystuen, A., et al. (2005). An enzymatic cascade of Rab5 effectors regulates phosphoinositide turnover in the endocytic pathway. J. Cell Biol. *170*, 607–618.

Stein, M.P., Feng, Y., Cooper, K.L., Welford, A.M., and Wandinger-Ness, A. (2003). Human VPS34 and p150 are Rab7 interacting partners. Traffic *4*, 754–771.

Tran, P.V., Haycraft, C.J., Besschetnova, T.Y., Turbe-Doan, A., Stottmann, R.W., Herron, B.J., Chesebro, A.L., Qiu, H., Scherz, P.J., Shah, J.V., et al. (2008). THM1 negatively modulates mouse sonic hedgehog signal transduction and affects retrograde intraflagellar transport in cilia. Nat. Genet. *40*, 403–410.

Vanhaesebroeck, B., Guillermet-Guibert, J., Graupera, M., and Bilanges, B. (2010). The emerging mechanisms of isoform-specific PI3K signalling. Nat. Rev. Mol. Cell Biol. *11*, 329–341.

Velichkova, M., Juan, J., Kadandale, P., Jean, S., Ribeiro, I., Raman, V., Stefan, C., and Kiger, A.A. (2010). Drosophila Mtm and class II PI3K coregulate a PI(3)P pool with cortical and endolysosomal functions. J. Cell Biol. *190*, 407–425.

Wang, J., Morita, Y., Mazelova, J., and Deretic, D. (2012). The Arf GAP ASAP1 provides a platform to regulate Arf4- and Rab11-Rab8-mediated ciliary receptor targeting. EMBO J. *31*, 4057–4071.

Westlake, C.J., Baye, L.M., Nachury, M.V., Wright, K.J., Ervin, K.E., Phu, L., Chalouni, C., Beck, J.S., Kirkpatrick, D.S., Slusarski, D.C., et al. (2011). Primary cilia membrane assembly is initiated by Rab11 and transport protein particle II (TRAPPII) complex-dependent trafficking of Rabin8 to the centrosome. Proc. Natl. Acad. Sci. USA *108*, 2759–2764.

Yoshimura, S., Egerer, J., Fuchs, E., Haas, A.K., and Barr, F.A. (2007). Functional dissection of Rab GTPases involved in primary cilium formation. J. Cell Biol. *178*, 363–369.

Yoshioka, K., Yoshida, K., Cui, H., Wakayama, T., Takuwa, N., Okamoto, Y., Du, W., Qi, X., Asanuma, K., Sugihara, K., et al. (2012). Endothelial PI3K-C2α, a class II PI3K, has an essential role in angiogenesis and vascular barrier function. Nat. Med. *18*, 1560–1569.

Zhang, X.M., Ramalho-Santos, M., and McMahon, A.P. (2001). Smoothened mutants reveal redundant roles for Shh and Ihh signaling including regulation of L/R symmetry by the mouse node. Cell *106*, 781–792.